DOI: 10.1002/eji.202048646 Eur. J. Immunol. 2021. 51: 138–150

Basic

European Journal of Immunology

Molecular immunology and signaling

Research Article

Evidence for an involvement of the ubiquitin-like modifier ISG15 in MHC class I antigen presentation

Tobias Held[1], *Michael Basler*[1,2], *Klaus-Peter Knobeloch*[3] *and Marcus Groettrup*[1,2]

[1] Division of Immunology, Department of Biology, University of Konstanz, Konstanz, Germany
[2] Biotechnology Institute Thurgau at the University of Konstanz, Kreuzlingen, Switzerland
[3] Institute of Neuropathology, University of Freiburg, Medical faculty, Freiburg, Germany

The IFN stimulated gene 15 (*ISG15*) encodes a 15-kDa ubiquitin-like protein, that is induced by type I IFNs and is conjugated to the bulk of newly synthesized polypeptides at the ribosome. ISG15 functions as an antiviral molecule possibly by being covalently conjugated to viral proteins and disturbing virus particle assembly. Here, we have investigated the effect of ISGylation on degradation and antigen presentation of viral and cellular proteins. ISGylation did not induce proteasomal degradation of bulk ISG15 target proteins neither after overexpressing ISG15 nor after induction by IFN-β. The MHC class I cell surface expression of splenocytes derived from ISG15-deficient mice or mice lacking the catalytic activity of the major de-ISGylating enzyme USP18 was unaltered as compared to WT mice. Fusion of ubiquitin or FAT10 to the long-lived nucleoprotein (NP) of lymphocytic choriomeningitis virus accelerated the proteasomal degradation of NP while fusion to ISG15 did not detectably speed up NP degradation. Nevertheless, MHC-I restricted presentation of two epitopes of NP were markedly enhanced when it was fused to ISG15 similarly to fusion with ubiquitin or FAT10. Thus, we provide evidence that ISG15 can enhance the presentation of antigens on MHC-I most likely by promoting co-translational antigen processing.

Keywords: antigen presentation · ISG15 · MHC class I · proteasome · ubiquitin-like modifier

Additional supporting information may be found online in the Supporting Information section at the end of the article.

Introduction

During a viral infection, type I IFNs play a central role in regulating the immune response through the induction of numerous IFN-stimulated genes (ISGs) (reviewed in [1]). IFN-stimulated gene 15 (*ISG15*) is one of the most highly [2] induced genes in response to a viral infection [3]. The antiviral activity of ISG15 was first observed during Sindbis virus infection [4]. Further studies found that ISG15 inhibited the growth of several other viruses (reviewed in [5,6]). These effects were reported to be caused by cytokine response regulation by ISG15 [7] or by regulating the host damage and repair response [8]. In addition, it has been shown that an antiviral role for ISG15 relies on its activation and covalent conjugation to its target proteins [9]. Studies suggested that conjugation of ISG15 to viral proteins can block oligomerization of these proteins, thereby disrupting the function and geometry of viral complexes [10]. ISG15 is a member of the ubiquitin (Ub) family and is composed of two ubiquitin-like domains that have

Correspondence: Dr. Marcus Groettrup
e-mail: Marcus.Groettrup@uni-konstanz.de

[The copyright line of this article was changed on 3 March 2021 after original online publication.]

structural homology to ubiquitin [11]. As a ubiquitin-like modifier, free ISG15 can be conjugated through a series of enzymatic reactions involving E1, E2, and E3 enzymes to lysine residues of target proteins similar to ubiquitin in a process referred to as ISGylation [11,12]. However, in contrast to Ub, ISG15 conjugation uses only a single E1 and E2 enzyme, namely Ube1L [13] and UbcH8 [14], as well as predominantly the E3 ligases HERC5 and HERC6 (LIT) in humans and mice, respectively [15,16]. HERC5 is associated with polyribosomes and was shown to ligate ISG15 to newly synthesized proteins, including viral proteins, which are the dominant proteins newly translated within an infected cell [17]. These results suggest that ISGylation in contrast to ubiquitylation has little to no target specificity [17] and viral proteins appear to be prominent targets of ISGylation during a viral infection. Ubiquitin and the ubiquitin-like modifier HLA-F-adjacent transcript 10 (FAT10) can target modified proteins for degradation by the 26S proteasome [18,19].

In contrast, the molecular effect of ISGylation on a target protein is still poorly understood. ISG15 has been reported to increase protein degradation by selective autophagy [20]. Furthermore, the formation of mixed chains of ubiquitin and ISG15 interferes with substrate degradation by the proteasome [21]. In contrast, it has also been reported that ISGylated p53 is degraded in a proteasome dependent manner [22]. For this reason, the molecular consequence of ISGylation and, thus, the cellular function of ISG15 with respect to protein degradation remains controversial. Since proteins modified by ubiquitin or the ubiquitin-like modifier FAT10 are degraded by the proteasome and generate peptides that will be loaded on MHC class-I molecules [23], we aimed to re-investigate the fate of ISGylated proteins. We show that ISGylation does not lead to proteasome dependent degradation of the bulk of ISGylated proteins. Hovever, ISG15-linkage upregulates antigen presentation of ISG15-fusion proteins, suggesting a novel role of ISG15 in antigen presentation.

Results

ISG15 conjugates are not degraded by the proteasome

The functional consequences of ISGylation regarding degradation of target proteins remain poorly understood and contradictory. For this reason, we aimed to clarify the fate of ISGylated proteins in terms of proteasomal degradation. Therefore, cycloheximide-chase experiments were performed in human HEK293T cells transiently transfected with plasmids encoding FLAG-ISG15 together with its cognate human E1 enzyme UBE1L (UBA7), its E2 enzyme UbcH8 (UBE2L6), and the major E3 ligase HERC5 (Fig. 1A). Moreover, endogenous mouse ISG15 was induced along with its E1/E2 and E3 enzymes in murine embryonic fibroblasts (MEFs) by stimulation with IFN-β (Fig. 1C) in order to examine the fate of ISGylated proteins. Western Blot analysis was performed to monitor the degradation of bulk ISGylated conjugates and free ISG15. In contrast to free and conjugated FAT10, which were both degraded in a proteasome dependent manner (Fig. 1B), no degradation of free ISG15 or ISG15 conjugates was detectable over the course of 5 h in neither of the two settings. For a more sensitive and longer lasting radioactive pulse-chase experiment with ^{35}S-methionine/cysteine, HEK293T cells were likewise transiently transfected with FLAG-ISG15 and E1/E2/E3 expression plasmids but again labeled ISG15 conjugates were not degraded even within 24 h, whereas free FLAG-ISG15 decreased over time (Fig. 1D). However, proteasome inhibition with MG132 did not rescue the degradation of free FLAG-ISG15. Interestingly, when the members of the conjugation cascade of ISG15 (UBE1L, UBCH8, HERC5) were not co-transfected in HEK293T cells, free FLAG-ISG15 remained stable over time in pulse-chase experiments (Fig. 1E). Of note, a minor amount of the singly expressed free FLAG-ISG15 appeared in the cell culture medium in accordance with earlier reports that ISG15 can be secreted [24,25]. Hence, the observed loss of free FLAG-ISG15 from cells over time (Fig. 1D) is probably due to secretion or de novo conjugation to substrate proteins rather than degradation. Taken together, these results show that the bulk of ISGylated proteins are not substantially degraded by the proteasome.

No fast proteasomal degradation of an ISG15-NP fusion protein

To further investigate the impact of ISG15 on the degradation rate, the fate of a single ISG15-linked protein rather than bulk ISGylated proteins was studied. To this aim, a plasmid encoding for ISG15 fused N-terminally to the rather long-lived nucleoprotein (NP) of lymphocytic choriomeningitis virus (LCMV) was generated [26]. Previously, we have shown that N-terminal fusion of ubiquitin (Ub) or FAT10 to LCMV-NP accelerated its degradation markedly [27]. Hence, the degradation kinetics of ISG15-NP was compared to those of Ub-NP, FAT10-NP, and NP alone in radioactive pulse-chase experiments after transient transfection of HEK293T cells. (Fig. 2A–D). In agreement with previous data, LCMV-NP was not detectably degraded over the chase time of five hours. While Ub-NP and FAT10-NP were rapidly degraded in a proteasome-dependent manner as evidenced by stabilization with MG132, radioactive ISG15-NP largely disappeared from the transfected cells over 5 h, but this loss could not at all be rescued by proteasome inhibition with MG132 (Fig. 2D). Interestingly, like FLAG-ISG15 (Fig. 1D, E), also the ISG15-NP fusion protein could be prominently detected in the supernatant after five hours of chase time (Fig. 2E), strongly suggesting secretion of ISG15NP rather than degradation.

MHC class I surface expression is downregulated in cells expressing high amounts of ISG15 conjugates

Previous studies showed an antiviral role for ISG15 that is mediated through ISGylation [9]. It was recently reported that ISG15 enhances MHC-class I antigen presentation [28]. Although ISGylated proteins are not degraded by the proteasome (Figs. 1 and 2), ISG15 can regulate cytokine responses [7] and upregulates IFN-γ

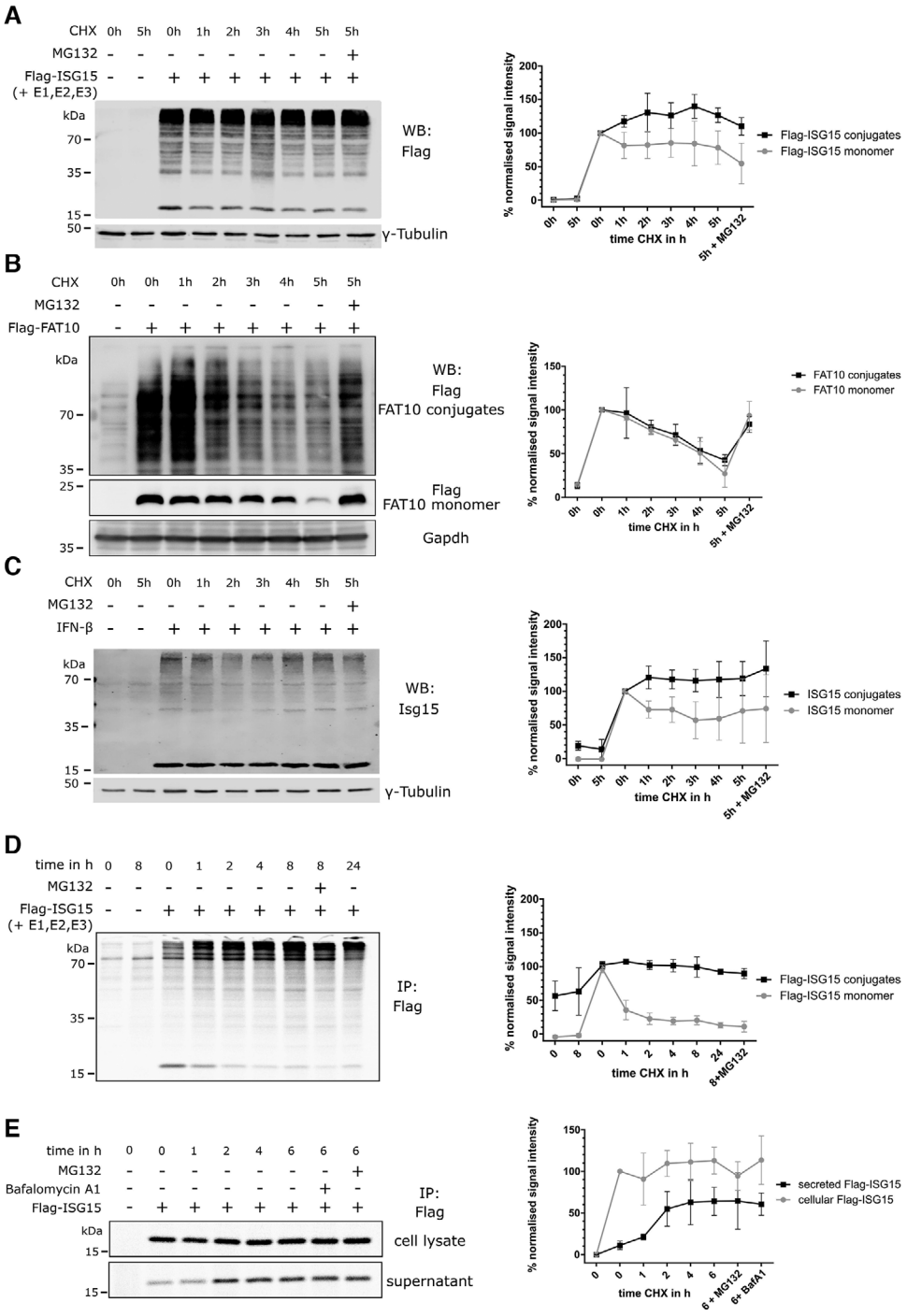

Figure 1. Kinetics of protein degradation in ISG15 overexpressing and IFN-β induced cells. (A) Cycloheximide (CHX) chase analysis of monomeric and conjugated FLAG-ISG15 after transient co-transfection of HEK293T cells with expression constructs for human FLAG-ISG15 and the E1 (UBE1L), E2 (UbcH8), and E3 (HERC5) enzymes of ISG15 (+ E1, E2, E3). (B) CHX chase analysis of monomeric and conjugated FLAG-FAT10 after transient co-transfection of HEK293T cells. (C) CHX chase analysis of endogenous monomeric and conjugated mouse ISG15 after IFN-β mediated ISG15 induction in mouse embryonic fibroblast (MEF) cells. Shown on the left are representative FLAG and mouse ISG15 western blots (WB). Proteasome activity was inhibited with 10 μM MG132 for indicated time periods of CHX chase. Quantification of the band intensity of ISG15 (separately for monomeric and conjugated form) after normalization to γ-tubulin used as loading control is shown on the right. (D and E) HEK293T cells overexpressing FLAG-ISG15 with (D) or without (E) ISGylation enzymes were labeled with ^{35}S-methionine/cysteine for 1 h. After labeling, samples were taken at indicated time points of chase and radioactive bands were visualized using a phosphorimager. Graphs (right side) show the quantification of FLAG-ISG15 signals (monomeric and conjugated form) as the mean ± SD derived from three independent experiments ($n = 3$). Where specified the medium was additionally supplemented with proteasome inhibitor MG132 (10 μM) or Bafilomycin A1 (BafA1) (0.1 μM). In western blot analysis GAPDH and γ-tubulin were used as loading controls. Representatives of three independent experiments are shown.

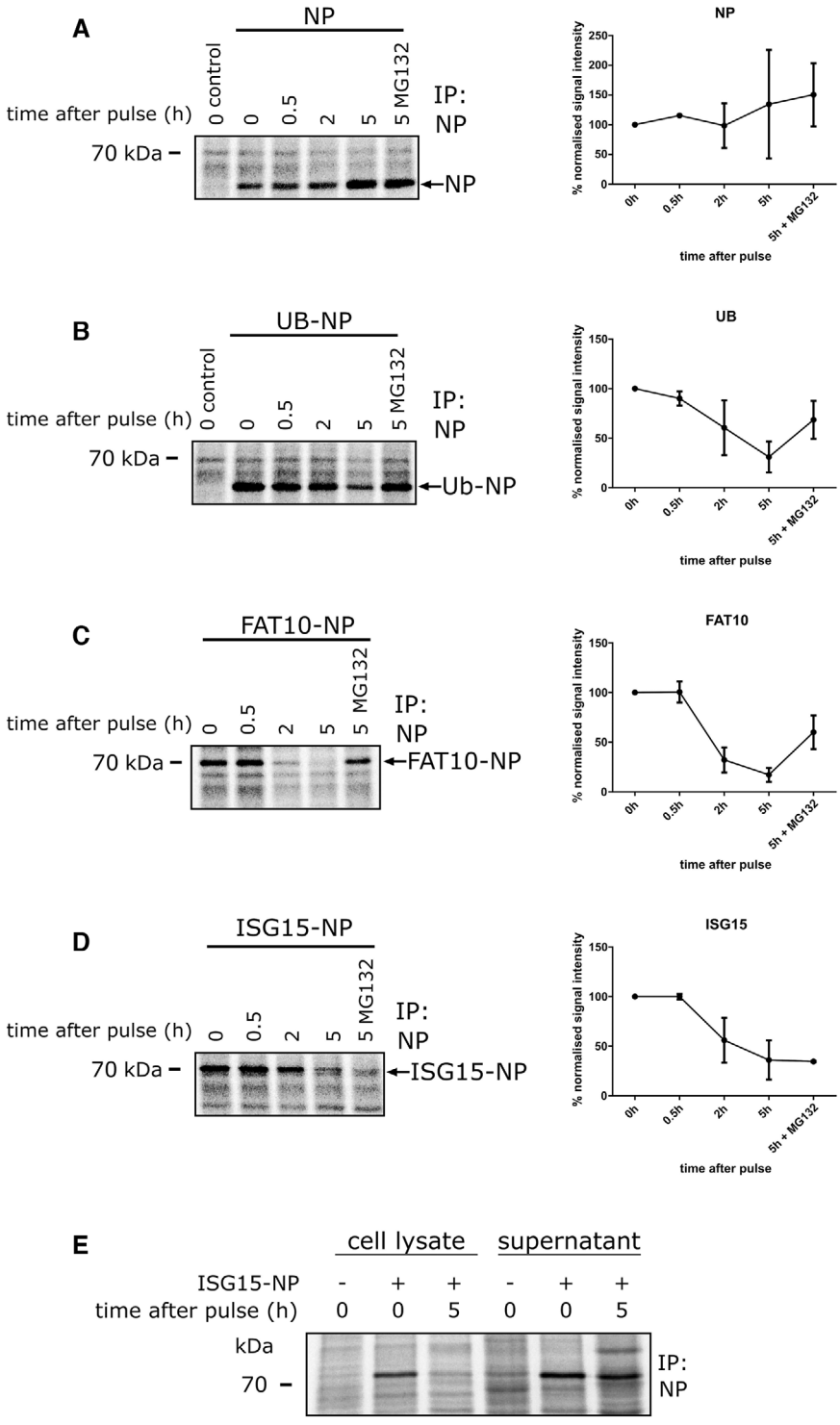

Figure 2. Degradation kinetics of radioactively labeled LCMV-NP and NP fusion proteins. The degradation of LCMV-NP (A) was compared to fusion proteins ubiquitin (Ub)-NP (B), FAT10-NP (C) as well as ISG15-NP (D). The proteins were overexpressed in HEK293T cells and ^{35}S-methionine/cysteine labeled for 1 h. After labeling, samples were taken at indicated time points of chase and used for immunoprecipitation using the NP specific antibody KL53. Radioactive proteins were visualized using a phosphorimager. Graphs (right side) show the mean value ± SD of indicated fusion protein signals derived from two independent experiments ($n = 2$). Representative autoradiograms are shown. Where indicated, proteasome activity was inhibited during the chase period with 10 μM MG132. (E) NP specific antibody KL53 was used to immunoprecipitate ISG15-NP from the cell culture supernatant of ^{35}S-methionine/cysteine labeled ISG15-NP transfected HEK293T cells. The experiment was performed three times, yielding similar results.

production [29]. Therefore, we wanted to re-examine whether ISG15 modifies antigen presentation by measuring MHC-I surface expression. HEK293T cells were transiently transfected with murine or human ISG15 with or without its cognate E1, E2, and E3 enzymes (Fig. 3A). An acid wash treatment was performed to remove MHC-I–peptide complexes from the cell surface (Supporting Information Fig. S1) and the re-appearance of MHC-I at the cell surface was determined by flow cytometry. Remarkably, we observed that in cells transfected with ISG15 in the presence of the conjugation machinery the reappearance of MHC-I molecules was slowed down significantly compared to control cells or cells transfected with ISG15 alone (Fig. 3). In accordance with previous observations [28], we found that cells expressing murine ISG15 displayed significantly higher MHC-I surface expression compared

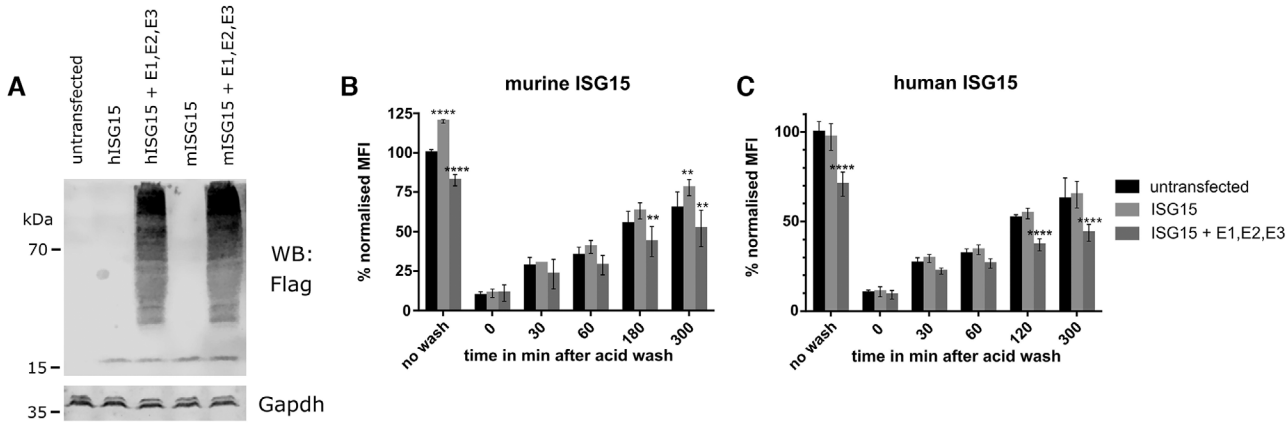

Figure 3. Altered MHC class I cell surface expression in ISG15 overexpressing HEK293T cells. HEK293T cells were transiently transfected with FLAG-ISG15 alone or together with expression constructs for ISGylation enzymes (E1, E2, E3). Additionally, cells were co-transfected with a plasmid encoding GFP to gate on transfected cells in flow cytometry experiments. Total human MHC-I surface expression was analysed by flow cytometry at indicated time points post acid wash treatment. Untreated (no wash) and untransfected cells served as a reference for maximal MHC-I surface expression and were set to 100 % of MHC-I surface expression. (A) FLAG-western blot analysis of HEK293T cells used for flow cytometric analysis 24 h post transfection to confirm the expression and conjugation of human (h) and murine (m) FLAG-ISG15. A representative blot of three independent experiments is shown. GAPDH was used as a loading control. (B and C) Reappearance of MHC class I molecules on the cell surface of cells overexpressing murine ISG15 (B) or human ISG15 (C) in the absence (ISG15) or presence (ISG15 + E1, E2, E3) of conjugation enzymes was analyzed by flow cytometry. Median fluorescence intensity (MFI) of HLA-A,B,C was normalized to the HLA-A,B,C expression of control cells. The full gating strategy is shown in Fig. S1. Data are presented as the mean ± SD from 3 independent experiments (n = 3). One-way ANOVA with Sidak's multiple comparison test, $^{*}p < 0.05$; $^{**}p < 0.01$; $^{***}p < 0.005$; $^{****}p < 0.0001$ was applied for data analysis.

to control cells 300 min after the acid wash (Fig. 3B). However, the biological relevance remains elusive. Furthermore, this effect was not observed in cells expressing human ISG15 (Fig. 3C). These data show that ISG15, at least when overexpressed, can modulate MHC-I surface expression.

Unchanged MHC-I surface expression in ISG15$^{-/-}$ and ISG15-deconjugation deficient mice

To further investigate a possible effect of ISG15 on class I surface expression but under in vivo conditions, the MHC-I surface expression on lymphocytes of C57BL/6, Isg15$^{-/-}$, and USP18C61A mice was analyzed. In USP18C61A mice, the gene encoding USP18 (also designated UBP43), which is the major ISG15 isopeptidase in vivo, is mutated at the active site cysteine to encode functionally inactive USP18C61A thus leading to increased levels of ISG15 conjugates in these mice [30]. The three mouse strains were intraperitoneally inoculated with 50 μg per mouse of the toll-like receptor 3 and RIG-I agonist polyinosinic:polycytidylic acid (polyI:C) to induce a type I IFN response and thereby ISG15 and its conjugation cascade [3]. ISG15 upregulation in the mice was confirmed in ISG15 Western Blots of splenocytes 24 h after polyI:C administration showing induction of monomeric ISG15 and ISG15 conjugates in WT mice, elevated ISG15 conjugate levels in USP18C61A mice and absence of ISG15 in splenocytes from ISG15$^{-/-}$ mice (Fig. 4A). Next, H-2K^{b} and H-2D^{b} cell surface expression was analyzed in T-cells (Fig. 4B), B-cells (Fig. 4C), dendritic cells (DCs) (Fig. 4D), macrophages (Fig. 4E), and NK cells (Fig. 4F) using flow cytometry (Supporting Information Fig. 2). Even though ISG15 expression and ISGylation had been strongly induced (Fig. 4A), no differences in H-2K^{b} and H-2D^{b} expression could be detected between ISG15$^{-/-}$, USP18C61A, and C57BL/6 mice. These data indicate that ISG15 and ISGylation do not alter the MHC class I expression under endogenous conditions in mice. Thus, a change of bulk MHC class I surface expression does not seem to contribute to the reported antiviral role of ISG15 in mice.

Increased proteasome-dependent presentation of NP epitopes after fusion of NP to ISG15

Since ISGylation modifies viral proteins at the ribosome [17,31–33] and since "defective ribosomal products (DRiPs)" or newly translated but rapidly degraded polypeptides contribute to MHC class I restricted antigen presentation [26,34], we further investigated a potential role of ISG15 in the generation of MHC-I ligands. Therefore, HEK293T cells stably expressing murine MHC molecules H-2L^{d} (Hek-L^{d}) or H-2D^{b} (Hek-D^{b}) (Supporting Information Fig. 3A and B) were transfected with constructs encoding for LCMV NP or the NP fusion proteins Ub-NP, Fat10-NP, and ISG15-NP (Fig. 2). One day post transfection, Hek-D^{b} or Hek-L^{d} cells were used to stimulate primary NP$_{396\text{-}404}$-specific CD8^{+} T-cell lines or splenocytes derived from LCMV infected BALB/c (H-2^{d}) mice, which mainly contain NP$_{118\text{-}126}$-specific CTLs. Presentation of the epitopes NP$_{396\text{-}404}$ (H-2D^{b}) and NP$_{118\text{-}126}$ (H-2L^{d}) was determined by double staining for CD8 and intracellular IFN-γ and analysis by flow cytometry (Supporting Information Fig. 3). In agreement with our previous report [27], presentation of NP$_{396\text{-}404}$ as well as NP$_{118\text{-}126}$ were significantly increased when LCMV-NP was N-terminally fused to degradation promoting ubiquitin or FAT10 as compared to cells stably expressing the

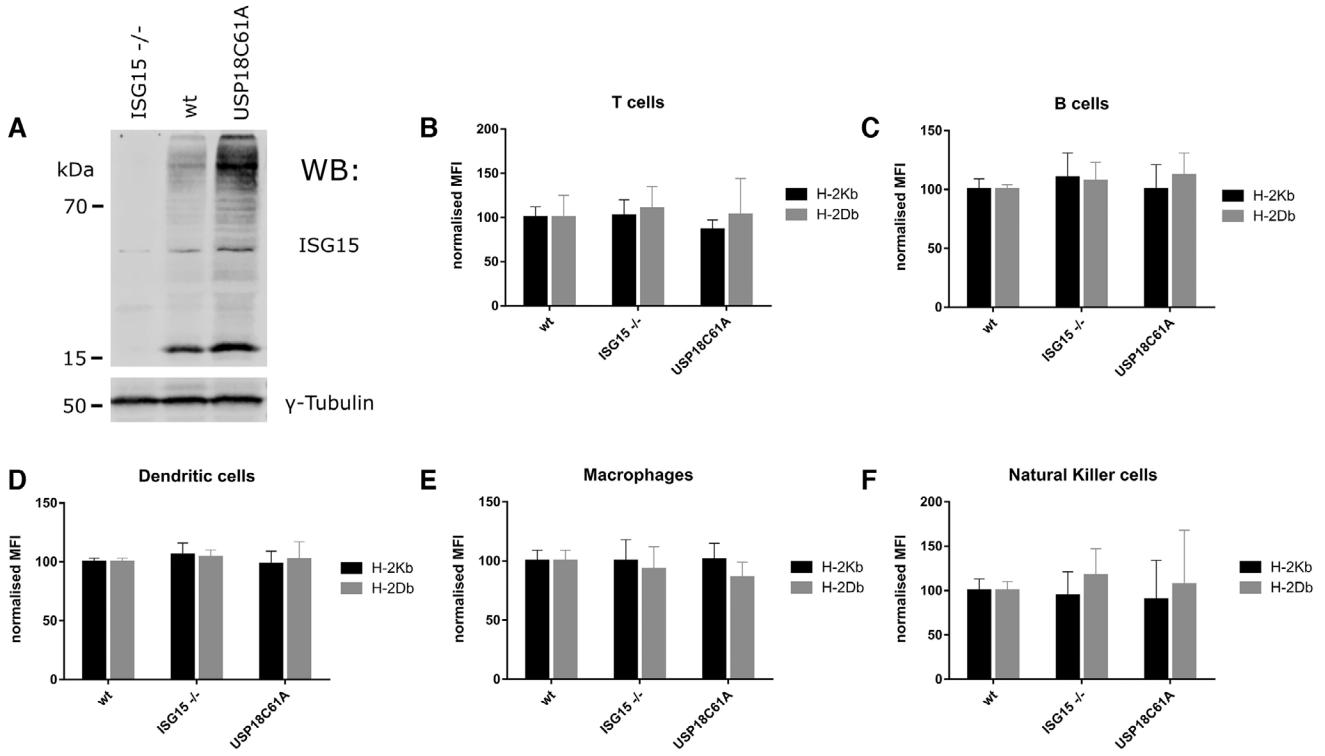

Figure 4. MHC class I cell surface expression of different splenocyte sub-population derived from WT, ISG15$^{-/-}$, and USP18C61A mice. ISG15 $^{-/-}$, USP18C61A, and C57BL/6 WT mice were treated with 50 μg polyinosinic:polycytidylic acid (poly I:C) for 24 h. (A) ISG15 western blot analysis of total splenocytes isolated from ISG15$^{-/-}$, USP18C61A, and C57BL/6 wt mice. γ-tubulin served as loading control. (B–F) Surface expression of MHC class I molecules H-2K^b and H-2D^b was analyzed in different immune cell subsets (CD3$^+$ (B), CD19$^+$ (C), CD11C$^+$ MHC II$^+$ (D), F4/80$^+$ (E), and CD3$^-$NK1.1$^+$ (F)) by flow cytometry. The full gating strategy is shown in Supporting Information Fig. S2. MFI of H-2K^b or H-2D^b was normalized to signals detected in cells of wt mice. Data are presented as the mean ± SD from 2 independent experiments. A representative blot of two independent experiments is shown. ISG15$^{-/-}$ $n = 3$, USP18C61A $n = 3$, C57BL/6 $n = 3$. Student's t-test, $^*p < 0.05$; $^{**}p < 0.01$; $^{***}p < 0.005$; $^{****}p < 0.0001$ was applied for data analysis.

long-lived unmodified NP (Fig. 5A and B). Unexpectedly, we observed the same increase in $NP_{118\text{-}126}$ and $NP_{396\text{-}404}$ presentation when NP was N-terminally fused to ISG15. To investigate the involvement of the proteasome, we repeated the experiment, acid washed the Hek-D^b and Hek-L^d cells, and additionally treated them with MG132 or BafA1 for 5 h prior to stimulation of specific CD8$^+$ T cells. We observed a significant decrease in presentation of NP epitopes fused to ubiquitin or FAT10 by treating cells with MG132 when compared to untreated cells (Fig. 6A and B). Interestingly the same effect was observed when ISG15-NP expressing cells were acid washed and treated with MG132, thus indicating involvement of the proteasome. Since fusion of ISG15 did not detectably accelerate proteasomal degradation of NP and since proteasome inhibition did not lead to an accumulation of ISG15-NP (Fig. 2D), we performed short term pulse chase experiments and investigated the degradation kinetic of radioactively labeled ISG15-NP over the chase time of 1 h (Fig. 6C). However, also in this setting neither accelerated degradation nor an effect of MG132 were detectable. Therefore, linkage to ISG15 might efficiently feed antigens into co-translational processing via a so far uncharacterized pathway that cannot be easily tracked with conventional degradation assays.

Mature ISG15$^{-/-}$ BM derived DC do not display significantly decreased antigen presentation

As ISG15 is upregulated during viral infections we aimed to investigate the effect ISG15 has on antigen presentation during a LCMV infection. Therefore, BM of C57BL/6 and ISG15$^{-/-}$ mice was isolated and matured BM derived DC (BMDC) were generated. Following a 5 h LCMV infection, the BMDC were used to present LCMV specific antigens to specific CD8$^+$ T-cell lines raised against the epitopes $NP_{396\text{-}404}$, $NP_{205\text{-}212}$ and against the glycoprotein (GP) epitope $GP_{33\text{-}41}$. Using Western Blot analysis, we found prominent ISG15 expression in all samples using BMDC derived from C57BL/6 mice, whereas BMDC derived from ISG15$^{-/-}$ mice were void of ISG15 (Fig. 7A). When antigen presentation of uninfected and LCMV infected BM derived DCs was assessed by IFN-γ intracellular cytokine staining, we observed an expected upregulation of antigen presentation when comparing the IFN-γ response of CD8$^+$ T cells of infected to uninfected cells for all tested epitopes (Fig. 7B–D). Yet, comparing infected BMDC from WT mice to those of ISG15$^{-/-}$ mice, only a tendency towards lower presentation by ISG15$^{-/-}$ BMDC especially of the $NP_{396\text{-}404}$ epitope but no significant differences in antigen presentation were observed.

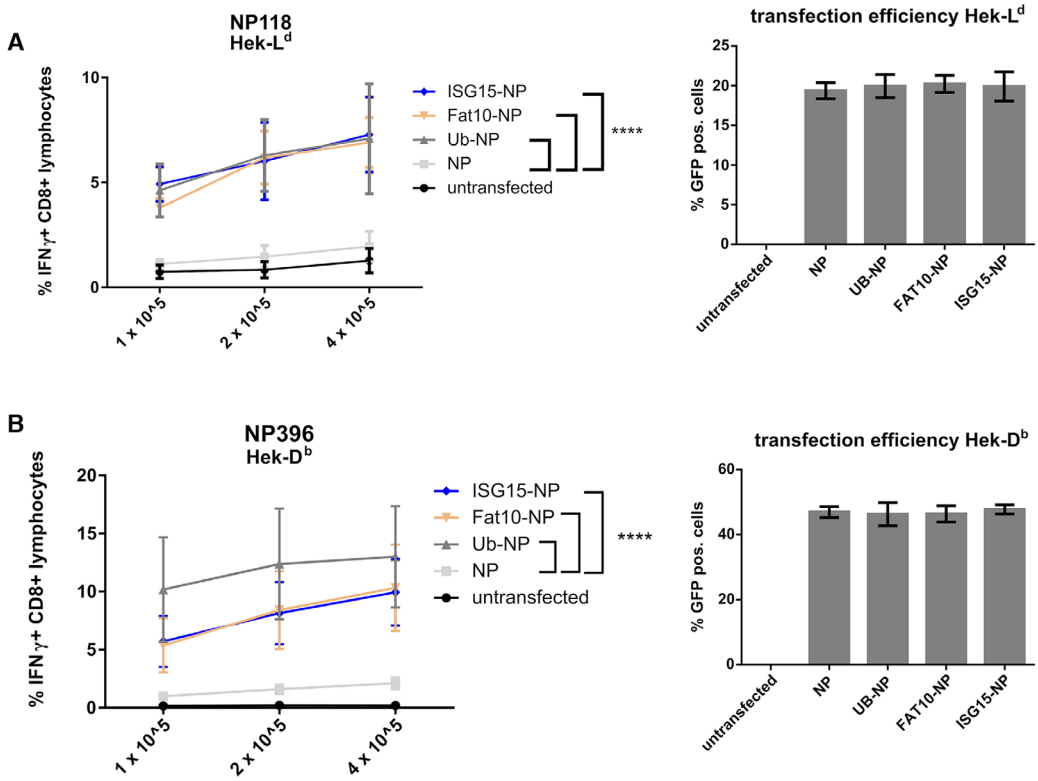

Figure 5. Fusion of ISG15 to NP increases antigen presentation of NP-derived epitopes. HEK293T cells stably expressing murine MHC class I molecules H-2L^d (A) or H-2D^b (B) were transfected with constructs encoding for LCMV NP or indicated NP fusion proteins. After 24 h, indicated numbers of cells were used to stimulate $NP_{118\text{-}126}$/H-2L^d - (A) or $NP_{396\text{-}404}$/H-2D^b (B) - specific CD8$^+$ T-cells. Activation of $NP_{118\text{-}126}$ - or $NP_{396\text{-}404}$ - specific CD8$^+$ T-cells was analyzed by staining for CD8 and intracellular IFN-γ. The percentages of IFN-γ-positive cells of CD8$^+$ cells are shown as determined by flow cytometry. The full gating strategy is shown in Supporting Information Fig. S3A. GFP co-transfection served as a control for transfection efficiency (right side). Pooled data of three independent experiments are presented as the mean ± SD ($n = 3$). One-way ANOVA with Sidak's multiple comparison test, $^*p < 0.05$; $^{**}p < 0.01$; $^{***}p < 0.005$; $^{****}p < 0.0001$ was applied for data analysis.

Discussion

The ubiquitin-like modifier ISG15 serves an important role in innate immune defense against infections with a broad range of viruses [5,6]. While several functions of ISG15 have been elucidated throughout the past decade, there are still mechanistic aspects of ISG15 action that remain to be determined. In particular, the functional consequences of ISG15 conjugation to proteins remain largely unknown and controversial. It is reported that ISG15 might simply disrupt the function of ISGylated proteins [35,36]. However, others showed that ISGylation is capable of negatively regulating the turnover of ubiquitylated proteins by the proteasome [37-39]. In contrast to this, it has also been reported that ISGylation directly targets some of its substrate proteins for degradation in a proteasome dependent manner [22]. The aim of this study was to elucidate the fate of ISGylated proteins in terms of proteasomal degradation, especially as other ubiquitin family modifiers such as ubiquitin and FAT10 target their modified protein substrates for degradation by the 26S proteasome [18,19]. In this respect parallels between ISG15 and FAT10 are noteworthy as both consist of two ubiquitin-like domains and both are massively induced by interferons i.e. ISG15 by IFNα/β and FAT10 by IFN-γ together with TNF-α. Moreover, ubiquitin, FAT10 and ISG15 modify newly translated proteins that can give rise to peptide ligands of MHC class I molecules [33].

In our experimental settings, we could demonstrate that conjugation of ISG15 does not target the bulk of its substrate proteins for efficient degradation by the proteasome (Fig. 1) regardless of using overexpressed (Fig. 1A and D) or type I IFN induced ISG15 (Fig. 1C). When addressing the same issue using LCMV NP fusion proteins we were able to confirm these findings (Fig. 2E). Interestingly, we did detect a decline of unconjugated ISG15 (Fig. 1D) as well as ISG15-NP signals over the course of time (Fig. 2D). This loss in signal was abrogated when the conjugation machinery of ISG15 was not co-transfected (Fig. 1D). Furthermore, we were able to immunoprecipitate unconjugated ISG15 (Fig. 1E) as well as ISG15-NP (Fig. 2E) from the cell culture supernatants. Therefore, the loss in signal is probably due to de novo conjugation or secretion rather than degradation.

Since Burks et al. recently published that intracellular unconjugated ISG15 might contribute to activation of the adaptive immune system by enhancing MHC-class I antigen presentation [28], we wanted to follow up on these findings. In accordance with their results, we observed a small but significant increase in MHC-I surface expression in ISG15 overexpressing cells (Fig. 3B). In contrast, a slight but again significant decrease in MHC-I surface

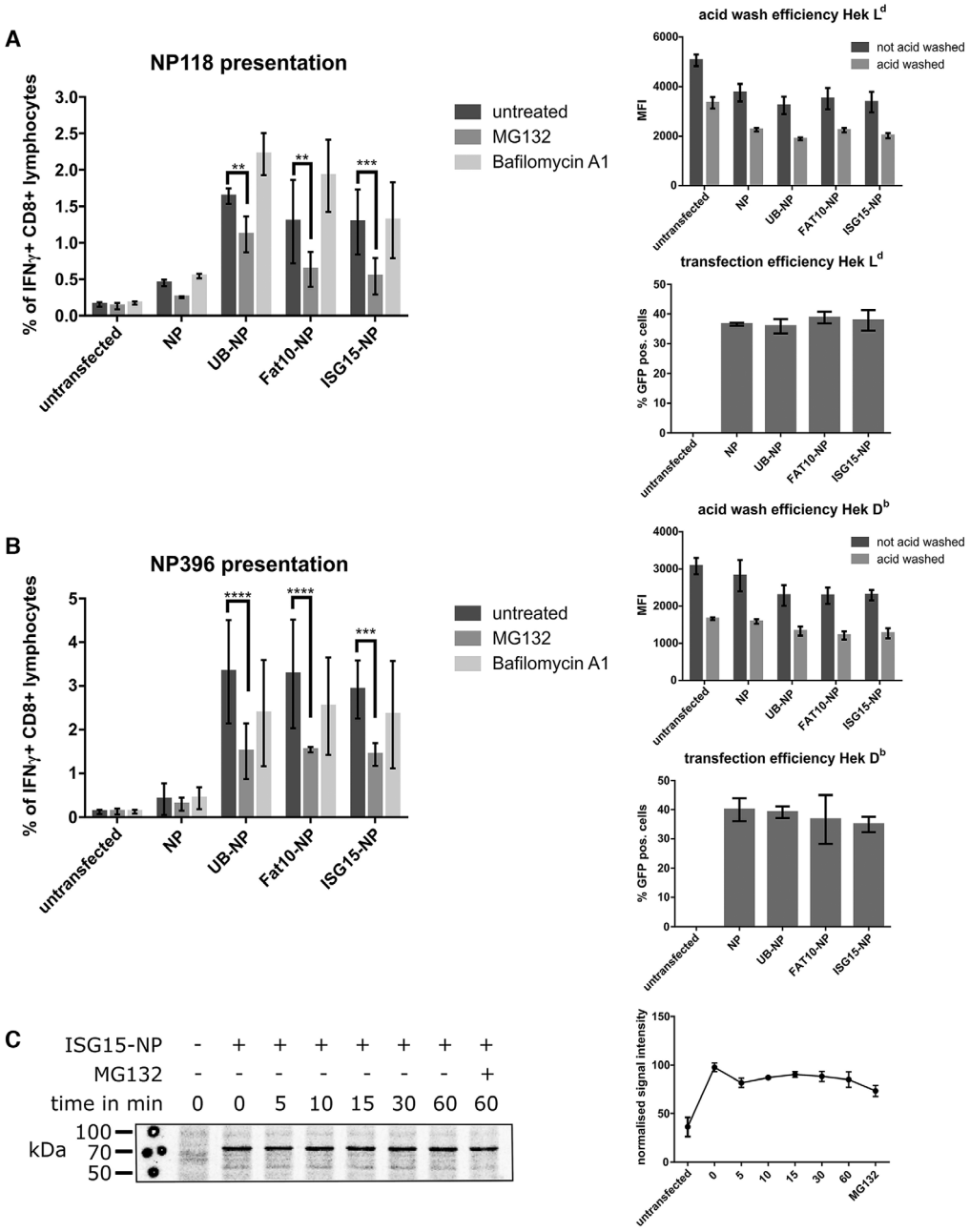

Figure 6. Proteasome inhibition decreases antigen presentation of ISG15-NP-derived epitopes. HEK293T cells stably expressing murine MHC class I molecules H-2L^d (A) or H-2D^b (B) were transfected with constructs encoding for LCMV NP or indicated NP fusion proteins. After 24 h, 2×10^5 cells were acid washed and treated with 10 μM MG132 or 0.1 μM BafA1 for 5 h. These cells were used to stimulate $NP_{118\text{-}126}$/H-2L^d- (A) or $NP_{396\text{-}404}$/H-2D^b- (B) specific CD8$^+$ T-cells. Activation of $NP_{118\text{-}126}$- or $NP_{396\text{-}404}$-specific CD8$^+$ T-cells was analyzed by staining for CD8 and intracellular IFN-γ. The percentages of IFN-γ-positive cells of CD8$^+$ cells are shown as determined by flow cytometry. GFP co-transfection served as a control for transfection efficiency and H-2L^d or H-2D^b staining as control for acid wash efficiency (right side). (C) HEK293T cells overexpressing ISG15-NP were labeled with ^{35}S-methionine/cysteine for 15 min. After labeling, samples were taken at indicated time points and radioactive bands were visualized using a phosphorimager. Pooled data of three independent experiments are presented as the mean ± SD ($n = 3$). One-way ANOVA with Sidak's multiple comparison test, $^*p < 0.05$; $^{**}p < 0.01$; $^{***}p < 0.005$; $^{****}p < 0.0001$ was applied for data analysis.

expression was detected in cells overexpressing ISG15 together with its conjugation enzymes (Fig. 3B, C). This decrease might be a result of conjugation of free ISG15 to unmodified substrate proteins or poly-ubiquitylated proteins which could interfere with their proteasomal degradation and consequently with the generation of MHC-I ligand peptides [21]. The differences in MHC-I surface expression that we observed compared to Burks et al. [28] when using human ISG15 (Fig. 3C) might be due to the different cell system used for the experiment. However, we were not able to detect any differences in the class I H-2D^b nor in the H-2K^b cell surface expression on splenocytes isolated from C57BL/6, ISG15$^{-/-}$, and USP18C61A mice one day after treatment with poly

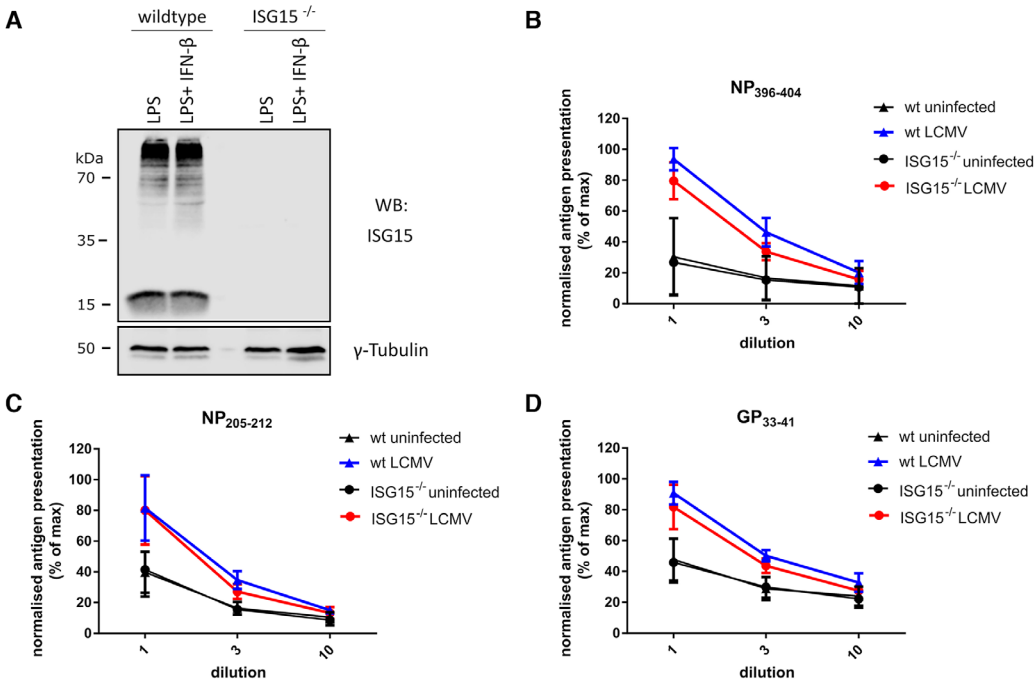

Figure 7. MHC class I antigen presentation by matured BMDCs. (A) Western blot analysis of ISG15 expression in murine matured WT and ISG15$^{-/-}$ BMDC. Cells were treated with 100 ng/mL LPS or LPS in combination with 1000 U/mL IFN-β for 1 day. A representative blot of three independent experiments is shown. γ-tubulin was used as a loading control. Uninfected and LCMV-WE infected BMDC were used to stimulate specific CD8$^+$ T-cell lines. Presentation of $NP_{396-404}$ (B), $NP_{205-212}$ (C), and GP_{33-41} (D) was determined by flow cytometry. The full gating strategy is shown in Supporting Information Fig. S3A. Effector to stimulator ratios of 1:1, 1:3 and 1:10 were used. Shown are IFN-γ responses of CD8$^+$ T cells normalized to the highest IFN-γ response. Pooled data of three independent experiments are presented as the mean ± SD ($n = 3$). Two-way ANOVA with Sidak's multiple comparison test, $^*p < 0.05$; $^{**}p < 0.01$; $^{***}p < 0.005$; $^{****}p < 0.0001$ was applied for data analysis.

I:C (Fig. 4B–F). Hence, the differences observed with the human embryonic kidney cell line HEK293T in vitro employing ISG15 overexpression could not be confirmed in vivo in mouse models.

The key finding of our study is that we found an increase in the presentation of the NP specific epitopes $NP_{396-404}$ and $NP_{118-126}$ in HEK293T cells expressing the fusion protein ISG15-NP as compared to unmodified NP (Fig. 5A and B). Similar results have previously been obtained with Ub-NP and FAT10-NP fusion proteins [27], which could be confirmed in this study. Ideally murine B8-D^b fibroblasts would have been used in addition to HEK293T cells to conduct the experiments shown in Figs. 5 and 6 [27]. Unfortunately, due to the low transfection efficiency and viability of B8-D^b cells after electroporation this experiment was not feasible. Nonetheless, the aforementioned finding is particularly interesting as FAT10 and Ub are known to target proteins for proteasomal degradation and thereby increase the peptide pool for MHC-I presentation [40,41] whereas an involvement of ISG15 in the generation of class I ligands has not yet been reported. Furthermore, a previous study of ISG15$^{-/-}$ mice found no significant alterations in the CTL response to LCMV at least when the immunodominant LCMV epitopes were analyzed together [42]. However, due to the ISG15 conjugation system being intimately tied to protein translation [17] it seems reasonable to hypothesize an involvement of ISGylated proteins in MHC-I antigen presentation, especially as most of the newly synthesized proteins during a viral infection will be viral proteins. We observed a significant decrease in MHC-I antigen presentation when acid washed and MG132 treated ISG15-NP overexpressing cells were used to present NP derived epitopes to specific CD8$^+$ T-cell lines (Fig. 6A and B). This finding strongly indicates the involvement of the proteasome in the ISG15-mediated generation of class I ligands. Nevertheless, in our CHX-chase and pulse-chase experiments we have not obtained evidence that conjugation or fusion of ISG15 to proteins accelerates their proteasomal degradation. It should be mentioned though that such assays have failed to show a proteasomal degradation of LCMV-NP even over days in spite of NP giving rise to the immunodominant class I epitopes $NP_{396-404}$ and $NP_{118-126}$ [26]. The demonstration that their presentation on class I relies on neosynthesis strongly suggests that these class I peptide ligands are generated from NP polypeptides shortly after or during their translation at the ribosome. This is a property of NP that is anticipated by the DRiP hypothesis [43]. Degradation of such polypeptides can occur within 30 min after their synthesis [44], however degradation analyses of ISG15-NP with ultra-short term pulse chase experiments did not reveal a role of ISG15 in targeting them for proteasomal degradation (Fig. 6C). Thus, presentation of ISG15-NP derived epitopes might be DRiP dependent [26]. In spite of major efforts, it has not been possible to experimentally monitor the degradation of DRiP subtrates up to date that may be due to extremely rapid degradation of DRiP polypeptides before the completion of synthesis. This could result in the failure of antibody binding to such newly translated polypeptides

thus interfering with their visualization. Nevertheless, when we addressed the effect of ISG15 on antigen presentation ex vivo by comparing LCMV infected BMDC from WT mice to those of ISG15$^{-/-}$ mice, only a tendency of reduction especially for the $NP_{396-404}$ epitope but no significant differences in antigen presentation were observed (Fig. 7B, C, D). Thus, this in vitro antigen presentation system failed to confirm an involvement of ISG15 in antigen presentation. Yet, a recent study by Nakashima et al. suggested that ISGylated proteins can be a target of lysosomal degradation. They suggest an involvement of ISG15 in p62-mediated aggresome formation and autophagic degradation of aggregates under conditions of cellular stress [20]. Peptides generated via this pathway could be cross-presented on MHC-I molecules [45] thereby circumventing the need for a proteasome dependent pathway. Less consistent with this hypothesis and aggregate formation of ISGylated proteins is the fact that we have observed secretion of soluble conjugated proteins (Fig. 2E). Moreover, p62 has also been shown to bind to the 26S proteasome and promote proteasomal degradation of protein substrates [46], which could play a role in a putative proteasome-dependent antigen targeting mechanism involving ISG15.

In summary, we could show that ISG15 can increase the amount of LCMV-NP peptide antigen presented on MHC-I molecules as potently as ubiquitin and FAT10 at least when N-terminally fused to NP. To show whether such an effect is also observed when ISG15 gets isopeptide-linked to antigens is technically much more challenging especially because the effect of ISGylation may be overruled by that of ubiquitylation or FAT10ylation. Nevertheless, first experimental evidence reported herein that ISG15 in addition to exerting direct antiviral and cytokine-like functions can also contribute to the class I antigen presentation pathway warrants further investigations in particular with respect to elucidating the underlying mechanisms.

Materials and Methods

Mice, cell lines, and media

C57BL/6 (H-2^b) and BALB/c (H-2^d) mice were originally obtained from Charles River Laboratories and further bred in the animal facilities of the University of Konstanz. Mice were kept in a specific pathogen-free facility in accordance with the rules of the veterinarian authority of Regierungspräsidium Freiburg. Isg15$^{-/-}$ and USP18C61A have been published previously [30, 42]. Animals were used at 8–10 weeks of age. To induce a type I IFN response, mice were i.p. inoculated with 50 μg poly I:C dissolved in 100 μL PBS.

The human embryonic kidney cell line HEK293T (ATCC, USA), Hek-D^b (Hek cells stably transfected with a plasmid encoding H-2D^b), Hek-L^d (Hek cells stably transfected with a plasmid encoding H-2L^d, kindly provided by A. Bitzer), and MEFs were cultured in DMEM with GlutaMAX™ supplemented with 10% FCS, 100 U/mL penicillin, and 100 μg/mL streptomycin. Culture media and supplements were obtained from Thermo Fisher Scientific (Germany) unless otherwise stated.

Generation of murine embryonic fibroblasts (MEFs)

The preparation of MEFs was performed as previously described [47].

Generation of ISG15-NP construct

The cloning of ISG15-NP was performed as previously described [27]. Shortly, NP was amplified by PCR from pCMV-NP [48] using the following primer pairs: 5'-TAT GAT GAA TTC ATG TCC TTG TCT AAGGAA GT-3' (forward) and 5'-ATC CCC GCG GCC GCT TAG AGT GTCACA ACA TT-3' (reverse). ISG15 was amplified by PCR from His_6-3xFLAG-ISG15 [35] using the following primer pairs: 5'-GTA CTA CTC GAG ATG TCG GTG TCA GAG CTG AAG-3' (forward) and 5'-TTA ATT GAA TTC GGC TAC CCG CAG GCG CAG ATT C-3' (reverse). Both fragments were digested with EcoRI, ligated, and introduced into the XhoI/NotI site of pCMV and the insert sequence was validated. Furthermore, a GG-to-VA mutation was introduced at the C-terminal end of the amino acid sequence of ISG15 to prevent cleavage of ISG15-NP.

Transfection and induction of cell lines

Transfection of HEK293T, Hek-D^b, and Hek-L^d cells was performed using TransIT®-LT1 Transfection Reagent (Mirus, Madison, WI, USA) according to the manufacturer's instruction with a 1:3 ratio of DNA to reagent. ISG15 expression in MEF cells was induced using 1000 U/mL IFN-β (PeproTech) for 24 h.

Cycloheximide chase experiment

For overexpression of ISG15, pcDNA3-His_6-3xFLAG-Isg15 [35] was transfected alone or together with pcDNA-UbcH8 [35], pcDNAUbe1L [35], and pcNTAPHerc5 [15]. A total DNA amount of 5 μg was used for transfection. Control cells were transfected with the same amount of DNA of an empty pcDNA3 plasmid. Hek293T cells or MEFs were treated 24 h after transfection with 50 μg/mL cycloheximide (CHX) over a course of 5 h. Samples were taken every hour, cells were pelleted and lysed using Ripa buffer [50 mM Tris, pH 7.5, 1 mM EDTA, 150 mM NaCl, 0.1% SDS, 1% NP-40, 1× protease inhibitor cocktail (complete Mini EDTA-free; Roche, Mannheim, Germany)] for 30 min on ice and lysates were cleared by centrifugation at 20000 × *g* for 15 min at 4°C. Samples were analyzed using SDS-PAGE and Western Blotting.

SDS-PAGE and western blotting

Cleared lysates were boiled with SDS sample buffer (50 mM Tris-HCl pH 6.8, 2% SDS, 10% glycerol, 20 mM dithiothreitol, 0.02

% bromophenol blue) for 5 min at 95°C. Proteins were separated by SDS-PAGE and blotted onto nitrocellulose membranes (Whatman). Membranes were blocked for 1 h using Intercept Blocking Buffer (LI-COR) and incubated with primary antibodies at 4°C over night. Following antibodies were used: Flag (F7425, Sigma), γ-tubulin (GTU-88, Sigma), and ISG15 (K.P. Knobeloch). Next, membranes were washed and incubated with appropriate secondary antibodies. Secondary antibodies used were: IRDye 680RD goat anti-mouse IgG and IRDye 800CW goat anti-rabbit IgG (both LI-COR). Afterwards proteins were visualized using Odyssey Fc Imaging System (LI-COR) and quantified using ImageStudio (Ver. 5.2, LI-COR).

Radiolabeling and pulse chase experiments

For overexpression of NP and NP-fusion constructs pCMV-NP, pCMV-Ub-NP [48], pCMV-FAT10-VA-NP [48] and pCMV-ISG15-VA-NP were used. A total DNA amount of 5 μg was used for transfection. Control cells were transfected with the same amount of DNA of an empty pCMV vector. HEK293T cells were starved 1 h in medium lacking cysteine and methionine (Sigma). After starvation cells were washed and radiolabeled for 1 h with ^{35}S-methionine/cysteine 24 h after transfection as previously described [27]. Next, radiolabeled cells were equally distributed in 6-well plates and further cultured in 1.5 mL of culture medium. One well was additionally supplemented with 10 μM MG132 to inhibit proteasome dependent degradation. Over the course of the chase, samples were taken at different time points. Cells were pelleted and lysed using Ripa buffer [50 mM Tris, pH 7.5, 1 mM EDTA, 150 mM NaCl, 0.1% SDS, 1% NP-40, 1 × protease inhibitor cocktail (complete Mini EDTA-free; Roche, Mannheim, Germany)] for 30 minutes on ice and lysates were cleared by centrifugation at 20000 x g for 15 minutes at 4°C. Radioactivity of cleared lysates was quantified using a scintillation counter (TOPcount NXT, Canberra Packard). Measured values were used to adjust supernatants to equal amounts of radioactivity before immunoprecipitation (IP) was performed overnight at 4°C. Proteins were separated by SDS-PAGE and gels were dried and exposed to a radiosensitive photo plate. 24 h later radioactive signals were visualized using a phosphor imager (Molecular Imager FX; Bio-Rad). Signals were quantified using ImageJ (Wayne Rasband, National Institutes of Health, Bethesda, MD, USA). For the IP of FLAG-ISG15 EZview™ Red ANTI-FLAG® M2 Affinity Gel beads (Sigma) were used and the IP of NP and NP fusion proteins was performed with EZview™ Red Protein G Affinity Gel beads (Sigma) pre-incubated with NP specific antibody KL53 [49]. To IP ISG15-NP from cell culture supernatant 1.5 mL supernatant was incubated with respective Affinity Gel beads.

Acid wash and MHC class I surface expression

HEK293T cells were transfected with pCDH-EF1a-mISG15-IRES-cGFP (kind gift of R. Schregle) for murine ISG15 and with pcDNA3-His$_6$-3xFLAG-ISG15 [35] for human ISG15 with and without pcDNA-UbcH8 [35], pcDNAUbe1L [35] and pcNTA-PHerc5 [15]. In the human setting and in experiments with NP fusion proteins pCDH-EF1a-IRES-cGFP (SystemBiosciences) was additionally transfected to enable gating on GFP positive cells. Control cells were transfected with the same amount of DNA of an empty pcDNA3 and pCDH-EF1a-IRES-cGFP vector. An acid wash treatment using citric acid buffer (0.131 M citric acid, 0.066 M NaH_2PO_4, pH 3) was performed with cells 24 h after transfection. Cells were washed twice with PBS and medium. Cells were further incubated in medium at 37°C. MHC class I surface expression was analyzed by flow cytometry. HEK293T cells were stained with anti-HLA-ABC (W6/32, eBioscience) antibody. To analyze H-2K^b and H-2D^b expression of splenocyte subsets from C57BL/6, ISG15$^{-/-}$ and USP18C61A mice, cells were stained with the following antibodies: anti-CD3ε (145-2C11), anti-CD19 (6D5), anti-CD11c (HL3), anti-MHC II (M5/114.15.2), anti-NK1.1 (PK136), anti-F4/80, (BM8), anti-H-2K^b (AF6-88.5.5.3, BioLegend), anti-H-2D^b (28-15-8) and fixable viability stain 780 (BD Bioscience). All antibodies were purchased from eBioscience unless indicated otherwise. Flow cytometry analyses was performed according to previously described guidelines [50]. Cells were acquired using a FACSVerse flow cytometer (BD Biosciences) and analyzed using FlowJo software (BD Biosciences).

Generation of specific CD8$^+$ T-cell lines

NP$_{396\text{-}404}$/H-2D^b-specific CD8$^+$ T-cell lines were generated in accordance with MIATA guidelines as previously described [27]. Splenocytes derived from LCMV-WE infected BALB/c mice (200 pfu; d8 post infection) were used ex vivo to detect presentation of NP$_{118\text{-}126}$ on H-2L^d.

In vitro antigen presentation assays and intracellular cytokine staining (ICS)

To determine the extent of direct presentation after transfection of NP-constructs the activation of CD8$^+$ T-cells was measured in an in vitro assay. Twenty-four hours post transfection, cells were either acid washed using citric acid buffer (0.131 M citric acid, 0.066 M NaH_2PO_4, pH 3) or kept untreated. Next, cells were treated with 10 μM MG132, 0.1 μM BafA1, or were left untreated for additional 5 h. Afterward, cells were seeded in a 96-well plate. NP-specific CD8$^+$ T-cell (2×10^5) and brefeldin A in a final concentration of 10 μg/mL were added. Samples were incubated for 5 h at 37°C before they were fixed using 4% paraformaldehyde and stained using the following antibodies: anti-CD8a (53-6.7), anti IFN-γ (XMG1.2), and fixable viability stain 780 (BD Bioscience). All antibodies were purchased from eBioscience unless indicated otherwise. Cells were acquired using a FACSVerse flow cytometer (BD Biosciences) and analyzed using FlowJo software (BD Biosciences). Flow cytometry analyses was performed according to previously described guidelines [50].

Generation of mature BMDCs

Bone marrow was isolated from C57BL/6 and ISG15$^{-/-}$ mice. Isolated BM was cultured for 6 days at 37°C in the presence of 20 ng/mL GM-CSF to generate immature BMDCs. BMDCs were matured in the presence of 100 ng/mL LPS and 1000 U/mL IFN-β for 1 day.

LCMV infection of mature BMDC

Mature BMDC were infected with LCMV-WE at an MOI of 10 for 5 h. Antigen presentation of infected mature BMDC was analyzed by using specific CD8$^+$ T-cell lines and subsequent IFN-γ intracellular cytokine staining.

Statistical analysis

For statistical analyses, groups from similar experiments were pooled and analyzed for significant differences as indicated in the graph. All statistical analyses were performed using GraphPad Prism software (version 6.04) (GraphPad, San Diego, CA). Error bars represent mean ± SD unless otherwise stated.

Acknowledgments: The authors thank Annegret Bitzer for contribution of the Hek-L^d cell line. The authors acknowledge the personnel of the Animal Research Facility of Konstanz University for animal care taking and the staff of the flow cytometry facility of the University of Konstanz (FlowKon) for help with flow cytometry. T.H. was supported by the InViTe Ph.D. program from the Baden-Wuerttemberg Ministry for Science, Research and Art (MWK Baden-Württemberg). This work was supported by Deutsche Forschungsgemeinschaft (DFG) Collaborative Research Center SFB969, project C01 and the DFG grant GR 1517/25-1 (to M.G.). Open access funding enabled and organized by Projekt DEAL.

Conflict of Interest: The authors declare no commercial or financial conflict of interest.

References

1 **Schneider, W. M., Chevillotte, M. D. and Rice, C. M.**, Interferon-stimulated genes: a complex web of host defenses. *Annu. Rev. Immunol.* 2014. **32**: 513–545.

2 **Der, S. D., Zhou, A., Williams, B. R. and Silverman, R. H.**, Identification of genes differentially regulated by interferon alpha, beta, or gamma using oligonucleotide arrays. *Proc. Natl. Acad. Sci. U. S. A.* 1998. **95**: 15623–15628.

3 **Sampson, D. L., Fox, B. A., Yager, T. D., Bhide, S., Cermelli, S., McHugh, L. C., Seldon, T. A. et al.**, A four-biomarker blood signature discriminates systemic inflammation due to viral infection versus other etiologies. *Sci. Rep.* 2017. **7**: 2914.

4 **Lenschow, D. J., Giannakopoulos, N. V., Gunn, L. J., Johnston, C., O'Guin, A. K., Schmidt, R. E., Levine, B. and Virgin, H. W. T.**, Identification of interferon-stimulated gene 15 as an antiviral molecule during Sindbis virus infection in vivo. *J. Virol.* 2005. **79**: 13974–13983.

5 **Hermann, M. and Bogunovic, D.**, ISG15: in sickness and in health. *Trends Immunol.* 2017. **38**: 79–93.

6 **Morales, D. J. and Lenschow, D. J.**, The antiviral activities of ISG15. *J. Mol. Biol.* 2013. **425**: 4995–5008.

7 **Werneke, S. W., Schilte, C., Rohatgi, A., Monte, K. J., Michault, A., Arenzana-Seisdedos, F., Vanlandingham, D. L.**, et al., ISG15 is critical in the control of Chikungunya virus infection independent of UbE1L mediated conjugation. *PLoS Pathog.* 2011. **7**: e1002322.

8 **Morales, D. J., Monte, K., Sun, L., Struckhoff, J. J., Agapov, E., Holtzman, M. J., Stappenbeck, T. S. and Lenschow, D. J.**, Novel mode of ISG15-mediated protection against influenza A virus and Sendai virus in mice. *J. Virol.* 2015. **89**: 337–349.

9 **Rahnefeld, A., Klingel, K., Schuermann, A., Diny Nicola, L., Althof, N., Lindner, A., Bleienheuft, et al.**, Ubiquitin-like protein ISG15 (Interferon-Stimulated Gene of 15 kDa) in host defense against heart failure in a mouse model of virus-induced cardiomyopathy. *Circulation* 2014. **130**: 1589–1600.

10 **Zhao, C., Sridharan, H., Chen, R., Baker, D. P., Wang, S. and Krug, R. M.**, Influenza B virus non-structural protein 1 counteracts ISG15 antiviral activity by sequestering ISGylated viral proteins. *Nat. Commun.* 2016. **7**: 12754.

11 **Haas, A. L., Ahrens, P., Bright, P. M. and Ankel, H.**, Interferon induces a 15-kilodalton protein exhibiting marked homology to ubiquitin. *J. Biol. Chem.* 1987. **262**: 11315–11323.

12 **Zhang, D. and Zhang, D. E.**, Interferon-stimulated gene 15 and the protein ISGylation system. *J. Interferon Cytokine Res.* 2011. **31**: 119–130.

13 **Narasimhan, J., Wang, M., Fu, Z., Klein, J. M., Haas, A. L. and Kim, J. J.**, Crystal structure of the interferon-induced ubiquitin-like protein ISG15. *J. Biol. Chem.* 2005. **280**: 27356–27365.

14 **Zhao, C., Beaudenon, S. L., Kelley, M. L., Waddell, M. B., Yuan, W., Schulman, B. A., Huibregtse, J. M. and Krug, R. M.**, The UbcH8 ubiquitin E2 enzyme is also the E2 enzyme for ISG15, an IFN-alpha/beta-induced ubiquitin-like protein. *Proc. Natl. Acad. Sci. U. S. A.* 2004. **101**: 7578–7582.

15 **Dastur, A., Beaudenon, S., Kelley, M., Krug, R. M. and Huibregtse, J. M.**, Herc5, an interferon-induced HECT E3 enzyme, is required for conjugation of ISG15 in human cells. *J. Biol. Chem.* 2006. **281**: 4334–4338.

16 **Wong, J. J., Pung, Y. F., Sze, N. S. and Chin, K. C.**, HERC5 is an IFN-induced HECT-type E3 protein ligase that mediates type I IFN-induced ISGylation of protein targets. *Proc. Natl. Acad. Sci. U. S. A.* 2006. **103**: 10735–10740.

17 **Durfee, L. A., Lyon, N., Seo, K. and Huibregtse, J. M.**, The ISG15 conjugation system broadly targets newly synthesized proteins: implications for the antiviral function of ISG15. *Mol. Cell* 2010. **38**: 722–732.

18 **Groettrup, M., Pelzer, C., Schmidtke, G. and Hofmann, K.**, Activating the ubiquitin family: UBA6 challenges the field. *Tr. Biochem. Sci.* 2008. **33**: 230–237.

19 **Schmidtke, G., Aichem, A. and Groettrup, M.**, FAT10ylation as a signal for proteasomal degradation. *Biochim. Biophys. Acta* 2014. **1843**: 97–102.

20 **Nakashima, H., Nguyen, T., Goins, W. F.** and **Chiocca, E. A.**, Interferon-stimulated gene 15 (ISG15) and ISG15-linked proteins can associate with members of the selective autophagic process, histone deacetylase 6 (HDAC6) and SQSTM1/p62. *J. Biol. Chem.* 2015. **290**: 1485–1495.

21 **Fan, J. B., Arimoto, K., Motamedchaboki, K., Yan, M., Wolf, D. A. and Zhang, D. E.**, Identification and characterization of a novel ISG15-ubiquitin mixed chain and its role in regulating protein homeostasis. *Sci. Rep.* 2015. **5**: 12704.

22 **Huang, Y. F., Wee, S., Gunaratne, J., Lane, D. P. and Bulavin, D. V.**, Isg15 controls p53 stability and functions. *Cell Cycle* 2014. **13**: 2200–2210.

23 **Rock, K. L. and Goldberg, A. L.**, Degradation of cell proteins and the generation of MHC class I-presented peptides. *Annu. Rev. Immunol.* 1999. **17**: 739–779.

24 **Swaim, C. D., Scott, A. F., Canadeo, L. A. and Huibregtse, J. M.**, Extracellular ISG15 signals cytokine secretion through the LFA-1 integrin receptor. *Mol. Cell* 2017. **68**: 581–590 e585.

25 **D'Cunha, J., Ramanujam, S., Wagner, R. J., Witt, P. L., Knight, E., Jr. and Borden, E. C.**, In vitro and in vivo secretion of human ISG15, an IFN-induced immunomodulatory cytokine. *J. Immunol.* 1996. **157**: 4100–4108.

26 **Khan, S., de Giuli, R., Schmidtke, G., Bruns, M., Buchmeier, M., van den Broek, M. and Groettrup, M.**, Cutting edge: neosynthesis is required for the presentation of a T cell epitope from a long-lived viral protein. *J. Immunol.* 2001. **167**: 4801–4804.

27 **Schliehe, C., Bitzer, A., van den Broek, M. and Groettrup, M.**, Stable antigen is most effective for eliciting CD8+ T-cell responses after DNA vaccination and infection with recombinant vaccinia virus in vivo. *J. Virol.* 2012. **86**: 9782–9793.

28 **Burks, J., Reed, R. E. and Desai, S. D.**, Free ISG15 triggers an antitumor immune response against breast cancer: a new perspective. *Oncotarget* 2015. **6**: 7221–7231.

29 **Bogunovic, D., Byun, M., Durfee, L. A., Abhyankar, A., Sanal, O., Mansouri, D., Salem, S.**, et al., Mycobacterial disease and impaired IFN-gamma immunity in humans with inherited ISG15 deficiency. *Science* 2012. **337**: 1684–1688.

30 **Ketscher, L., Hannss, R., Morales, D. J., Basters, A., Guerra, S., Goldmann, T., Hausmann, A.**, et al., Selective inactivation of USP18 isopeptidase activity in vivo enhances ISG15 conjugation and viral resistance. *Proc. Natl. Acad. Sci. U. S. A.* 2015. **112**: 1577–1582.

31 **Takeuchi, T., Inoue, S. and Yokosawa, H.**, Identification and Herc5-mediated ISGylation of novel target proteins. *Biochem. Biophys. Res. Commun.* 2006. **348**: 473–477.

32 **Malakhov, M. P., Kim, K. I., Malakhova, O. A., Jacobs, B. S., Borden, E. C. and Zhang, D. E., High-throughput immunoblotting**. Ubiquitiin-like protein ISG15 modifies key regulators of signal transduction. *J. Biol. Chem.* 2003. **278**: 16608–16613.

33 **Spinnenhirn, V., Bitzer, A., Aichem, A. and Groettrup, M.**, Newly translated proteins are substrates for ubiquitin, ISG15, and FAT10. *FEBS Lett.* 2017. **591**: 186–195.

34 **Dolan, B. P., Bennink, J. R. and Yewdell, J. W.**, Translating DRiPs: progress in understanding viral and cellular sources of MHC class I peptide ligands. *Cell Mol. Life Sci.* 2011. **68**: 1481–1489.

35 **Zhao, C., Denison, C., Huibregtse, J. M., Gygi, S. and Krug, R. M.**, Human ISG15 conjugation targets both IFN-induced and constitutively expressed proteins functioning in diverse cellular pathways. *Proc. Natl. Acad. Sci. U. S. A.* 2005. **102**: 10200–10205.

36 **Jeon, Y. J., Choi, J. S., Lee, J. Y., Yu, K. R., Kim, S. M., Ka, S. H., Oh, K. H., Kim, K. I., Zhang, D. E., Bang, O. S. and Chung, C. H.**, ISG15 modification of filamin B negatively regulates the type I interferon-induced JNK signalling pathway. *EMBO Rep.* 2009. **10**: 374–380.

37 **Liu, M., Li, X. L. and Hassel, B. A.**, Proteasomes modulate conjugation to the ubiquitin-like protein, ISG15. *J. Biol. Chem.* 2003. **278**: 1594–1602.

38 **Desai, S. D., Haas, A. L., Wood, L. M., Tsai, Y. C., Pestka, S., Rubin, E. H., Saleem, A.**, et al., Elevated expression of ISG15 in tumor cells interferes with the ubiquitin/26S proteasome pathway. *Cancer Res.* 2006. **66**: 921–928.

39 **Ganesan, M., Poluektova, L. Y., Tuma, D. J., Kharbanda, K. K. and Osna, N. A.**, Acetaldehyde Disrupts Interferon Alpha Signaling in Hepatitis C Virus-Infected Liver Cells by Up-Regulating USP18. *Alcohol. Clin. Exp. Res.* 2016. **40**: 2329–2338.

40 **Michalek, M. T., Grant, E. P., Gramm, C., Goldberg, A. L. and Rock, K. L.**, A role for the ubiquitin-dependent proteolytic pathway in MHC class I-restricted antigen presentation. *Nature* 1993. **363**: 552–554.

41 **Ebstein, F., Lehmann, A. and Kloetzel, P. M.**, The FAT10- and ubiquitin-dependent degradation machineries exhibit common and distinct requirements for MHC class I antigen presentation. *Cell Mol. Life Sci.* 2012. **69**: 2443–2454.

42 **Osiak, A., Utermöhlen, O., Niendorf, S., Horak, I. and Knobeloch, K.-P.**, ISG15, an Interferon-Stimulated Ubiquitin-Like Protein, Is Not Essential for STAT1 Signaling and Responses against Vesicular Stomatitis and Lymphocytic Choriomeningitis Virus. *Mol. Cell. Biol.* 2005. **25**: 6338–6345.

43 **Yewdell, J. W., Anton, L. C. and Bennink, J. R.**, Defective ribosomal products (DRiPs): a major source of antigenic peptides for MHC class I molecules? *J. Immunol.* 1996. **157**: 1823–1826.

44 **Schubert, U., Anton, L. C., Gibbs, J., Norbury, C. C., Yewdell, J. W. and Bennink, J. R.**, Rapid degradation of a large fraction of newly synthesized proteins by proteasomes. *Nature* 2000. **404**: 770–774.

45 **English, L., Chemali, M., Duron, J., Rondeau, C., Laplante, A., Gingras, D., Alexander, D., Leib, D., Norbury, C., Lippe, R. and Desjardins, M.**, Autophagy enhances the presentation of endogenous viral antigens on MHC class I molecules during HSV-1 infection. *Nat. Immunol.* 2009. **10**: 480–487.

46 **Seibenhener, M. L., Babu, J. R., Geetha, T., Wong, H. C., Krishna, N. R. and Wooten, M. W.**, Sequestosome 1/p62 is a polyubiquitin chain binding protein involved in ubiquitin proteasome degradation. *Mol. Cell Biol.* 2004. **24**: 8055–8068.

47 **Bitzer, A., Basler, M., Krappmann, D. and Groettrup, M.**, Immunoproteasome subunit deficiency has no influence on the canonical pathway of NF-kappaB activation. *Mol. Immunol.* 2017. **83**: 147–153.

48 **Rodriguez, F., Zhang, J. and Whitton, J. L., DNA immunization**: ubiquitination of a viral protein enhances cytotoxic T-lymphocyte induction and antiviral protection but abrogates antibody induction. *J. Virol.* 1997. **71**: 8497–8503.

49 **Shen, L. and Rock, K. L.**, Cellular protein is the source of cross-priming antigen in vivo. *Proc. Natl. Acad. Sci. U. S. A.* 2004. **101**: 3035–3040.

50 **Cossarizza, A., Chang, H. D., Radbruch, A., Acs, A., Adam, D., Adam-Klages, S., Agace, W. W.**, et al., Guidelines for the use of flow cytometry and cell sorting in immunological studies (second edition). *Eur. J. Immunol.* 2019. **49**: 1457–1973.

Abbreviations: **BMDC**: BM derived dendritic cells · **FAT10**: HLA-F adjacent transcript 10 · **ISG15**: IFN stimulated gene 15 · **Ub**: ubiquitin · **MEF**: murine embryonal fibroblasts · **LCMV**: lymphocytic choriomeningitis virus · **NP**: nucleoprotein

Full correspondence: Prof. Dr. Marcus Groettrup, Division of Immunology, Department of Biology, University of Konstanz, Universitaetsstrasse 10, D-78457 Konstanz, Germany
e-mail: Marcus.Groettrup@uni-konstanz.de

The peer review history for this article is available at https://publons.com/publon/10.1002/eji.202048646

Received: 20/3/2020
Revised: 16/6/2020
Accepted: 14/7/2020
Accepted article online: 20/7/2020